Fermi National Accelerator Laboratory

FERMILAB-Pub-92/266-E

Measurement of the $\gamma\gamma$ Partial Width of the χ_2 Charmonium Resonance

T.A. Armstrong et al
The Fermilab E760 Collaboration

Fermi National Accelerator Laboratory, Batavia, Illinois 60510

November 1992

Submitted to *Physical Review Letters*

Operated by Universities Research Association Inc. under Contract No. DE-AC02-76CHO3000 with the United States Department of Energy

Disclaimer

FERMILAB-Pub-92/266-E

Measurement of the $\gamma\gamma$ Partial Width of the χ_2 Charmonium Resonance

T.A. Armstrong[6], D. Bettoni[2], V. Bharadwaj[1], C. Biino[7], G. Borreani[2], D. Broemmelsiek[4], A. Buzzo[3], R. Calabrese[2], A. Ceccucci[7], R. Cester[7], M. Church[1], P. Dalpiaz[2], P.F. Dalpiaz[2], R. Dibenedetto[7], D. Dimitroyannis[5], M. Fabbri[2], J. Fast[4], A. Gianoli[2], C.M. Ginsburg[5], K. Gollwitzer[4], A. Hahn[1], M.A. Hasan[6], S. Hsueh[1], R. Lewis[6], E. Luppi[2], M. Macrí[3], A.M. Majewska[6], M. Mandelkern[4], F. Marchetto[7], M. Marinelli[3], J. Marques[4], W. Marsh[1], M. Martini[2], M. Masuzawa[5], E. Menichetti[7], A. Migliori[7], R. Mussa[7], S. Palestini[7], M. Pallavicini[3], N. Pastrone[7], C. Patrignani[3], J. Peoples Jr.[1], L. Pesando[7], F. Petrucci[2], M.G. Pia[3], S. Pordes[1], P.A. Rapidis[1], R. Ray[5,1], J. Reid[6], G. Rinaudo[7], B. Roccuzzo[7], J. Rosen[5], A. Santroni[3], M. Sarmiento[5], M. Savrie'[2], A. Scalisi[3], J. Schultz[4], K.K. Seth[5], A. Smith[4], G.A. Smith[6], M. Sozzi[7], S. Trokenheim[5], M.F. Weber[4], S. Werkema[1], Y. Zhang[6], J. Zhao[5], G. Zioulas[4].

(E-760 Collaboration)

[1] *Fermi National Accelerator Laboratory, Batavia, Illinois 60510, U.S.A.*
[2] *I.N.F.N. and University of Ferrara, 44100 Ferrara, Italy*
[3] *I.N.F.N. and University of Genoa, 16146 Genoa, Italy*
[4] *University of California at Irvine, California 92717, U.S.A.*
[5] *Northwestern University, Evanston, Illinois 60208, U.S.A.*
[6] *Pennsylvania State University, University Park, Pennsylvania 16802, U.S.A.*
[7] *I.N.F.N. and University of Turin, 10125 Turin, Italy.*

The E760 collaboration at Fermilab has studied the reaction $\bar{p}p \rightarrow \chi_2 \rightarrow \gamma\gamma$. We obtain values for the branching ratio and partial width to two photons of $BR(\chi_2 \rightarrow \gamma\gamma) = (1.54 \pm 0.47) \times 10^{-4}$ and $\Gamma(\chi_2 \rightarrow \gamma\gamma) = (0.304 \pm 0.097)\ KeV$.

PACS numbers : 14.40.Gx, 13.20.Gd, 13.75.Cs

This paper reports a measurement of the $\gamma\gamma$ decay of the χ_2 ($^3P_2$) charmonium resonance formed in $\bar{p}p$ annihilation. Within the framework of perturbative QCD [1], the ratio of the partial widths $\Gamma(\chi_2 \rightarrow gg)/\Gamma(\chi_2 \rightarrow \gamma\gamma)$ can be used to obtain a value for the coupling constant α_s at the charm quark mass.

Experiment E760 utilizes an internal hydrogen gas jet target which intersects a cooled beam of antiprotons circulating in the accumulator ring at Fermilab. The size of the interaction region is determined transversely by the beam size, 6 mm diameter, and longitudinally by the gas jet size, 6.3 mm for 95% containment. The detector [2] is optimized for the identification of the $e^+e^- + X$ and multi-γ final states. It covers the complete azimuth (ϕ) and the polar angle (θ) from 2° to 70°. It consists of two sets of scintillator hodoscopes (H1, H2), a forward charged particle veto (FCV), a multicell threshold Čerenkov counter for electron identification, several layers of charged tracking detectors, and central (CCAL) and forward (FCAL) electromagnetic calorimeters.

For the identification of the $\gamma\gamma$ final state the central calorimeter [3] is the essential part of the detector. It must distinguish between $\gamma\gamma$ events and the large background from hadronic processes - in particular $\bar{p}p \rightarrow \pi^0\pi^0$, $\bar{p}p \rightarrow \pi^0\gamma$, and $\bar{p}p \rightarrow \pi^0\eta$ - which have cross sections up to 10^3 times that of the $\gamma\gamma$ channel. The 1280 module lead glass Čerenkov counter array, 20 counters in θ by 64 counters in ϕ, is arranged in a pointing geometry and covers the region $11° \leq \theta \leq 70°$. The average rms angular resolution is 7 $mrad$ in θ and 11 $mrad$ in ϕ. The average rms energy resolution is $6.0\%/\sqrt{E(GeV)} + 1.4\%$.

E760 has collected a total integrated luminosity of 2.58 pb^{-1} at the χ_2 formation energy, $\sqrt{s} = 3556$ MeV. The $\gamma\gamma$ background is measured using 23.3 pb^{-1} of data taken at various values of $\sqrt{s}$ from 3523 MeV to 3686 MeV where resonant $\gamma\gamma$ production is not expected.

The luminosity is obtained by counting recoil protons from forward elastic scattering with silicon detector located at $\theta = 86.5°$. The luminosity is extracted from knowledge of the $\bar{p}p$ elastic cross section and the detector acceptance. The estimated error in the absolute luminosity, ± 4%, is included as a systematic error in this measurement.

The trigger for the experiment consists of two levels. At the hardware level a topological trigger requires at least two energetic clusters in the central calorimeter separated by $\geq 90°$ in azimuth (PBG1) [4]. Events with charged particles are vetoed by requiring no hits in the H1 or FCV scintillation counters. The calorimeter data are read into online processors which compute the invariant masses of all "photon" pairs ($M_{\gamma\gamma}$) and the total energy deposited in the calorimeters. Events with any $M_{\gamma\gamma} \geq 2.0$ GeV/c^2 are recorded on tape.

There are two sources of inefficiency in the trigger. The first comes from the PBG1 requirement and the other from the random veto of neutral events due to the high rate of charged particles in the scintillator counters. The PBG1 efficiency is found to be $> 98\%$ from analysis of $\bar{p}p \rightarrow J/\psi \rightarrow e^+e^-$ events collected with a trigger which uses only the hodoscope and Čerenkov data. The inefficiency due to the charged particle veto is measured by removing the veto requirement from the trigger, reconstructing $\bar{p}p \to \pi^0\pi^0$ events, and determining how often the trigger bits for the vetoes are set (with a correction for Dalitz decays and conversions in the beam pipe). The data used to measure this inefficiency were collected with an instantaneous luminosity of $3.5 \times 10^{30}\ cm^{-2}s^{-1}$ while the data used in the $\chi_2 \to \gamma\gamma$ analysis were collected at luminosities in the range $2.5 - 6.2 \times 10^{30}\ cm^{-2}s^{-1}$. The cross section for $\gamma\gamma$ candidates (after preliminary cuts) binned by instantaneous luminosity shows no luminosity dependence at the few percent level. We include a 3% systematic error in the trigger efficiency, and a comparable error in the analysis efficiency, to provide for possible luminosity dependence. The trigger efficiency is determined to be $\epsilon_{\text{trigger}} = 0.91 \pm 0.03 \pm 0.03$.

Offline, the central calorimeter clustering algorithm looks for local maxima (blocks with more energy than their eight nearest neighbors) and forms 3 by 3 clusters around these. Energy thresholds of 5 MeV for the central blocks and 20 MeV for the 9 block regions are used. For some events spurious clusters are formed, primarily due to the tails of signals from previous interactions. To identify such clusters 160 signals (20 in θ by 8 in ϕ), used primarily for triggering, are discriminated and latched with a narrow time gate (30 nsec). This system allows for accurate classification of clusters above 200 MeV as in-time or out-of-time, while below this energy they remain undetermined.

The cluster position is determined from a parameterization of the shower profile using the sum of two exponentials. When two clusters overlap the energy of the blocks in the overlapping region is shared between them using an iterative procedure. The fraction of energy assigned to each shower is based on the shower profile parameterizations, and the procedure is iterated until the shower centroids and shower energies are stable at the level of the intrinsic detector resolution.

The major sources of background to the $\gamma\gamma$ signal are $\pi^0\pi^0$ and $\pi^0\gamma$ events in which the π^0 decay is either nearly symmetric or highly asymmetric. Symmetric decays produce showers which can be mistaken for single photon showers. In order to identify such cases a *mass* is calculated for each shower,

$$m = \sqrt{\left(\sum_i E_i\right)^2 - \left(\sum_i \vec{p_i}\right)^2} \tag{1}$$

where E_i is the energy deposited in the i^{th} block, $\vec{p_i} = E_i\hat{x}_i$, and $\hat{x}_i$ is the unit vector from the interaction point to the center of the i^{th} block. Showers from symmetric π^0 decays have large *mass* values while those from single photons (or electrons) do not. Any shower with $m \geq 100\ MeV/c^2$ is split into two clusters, each representing an individual photon from the π^0. Fig. 1 shows the *mass* distributions for showers from J/ψ electrons and for showers from $\bar{p}p \to \pi^0\pi^0$ events. The low *mass* showers from π^0s in Fig. 1 are due to photons which are well separated in the calorimeter. Comparison of $\bar{p}p \to \pi^0\pi^0$ data with a Monte Carlo simulation indicates that the efficiency for identification of symmetric π^0 decays based on the *mass* cut is better than 99%.

The $\gamma\gamma$ analysis begins with events with two central calorimeter clusters with invariant mass $M_{\gamma\gamma} \geq 2.5\ GeV/c^2$. Up to two additional low energy clusters, classified as out-of-time or undetermined, are allowed in the central calorimeter. No clusters are allowed in the forward calorimeter. A 4C kinematical fit to the $\gamma\gamma$ hypothesis is done and events with a fit probability $CL \leq 5 \times 10^{-3}$ are rejected. An invariant mass cut at $\pm 10\% \sqrt{s}$ is imposed, corresponding to 3σ of the mass resolution as inferred from $J/\psi \rightarrow e^+e^-$ and $\psi' \rightarrow e^+e^-$ events. The masses calculated by pairing any additional low energy clusters with each of the high energy clusters associated with the $\gamma\gamma$ candidate are plotted in Fig. 2. Events with any mass in the π^0 ($80 - 170\ MeV/c^2$) or η ($410-690\ MeV/c^2$) window are rejected. The inset in Fig. 2 shows the η mass region after the removal of events with a π^0, indicating that there is a small contribution of events with an η.

Fig. 3 shows the center of mass angular distributions for the remaining $\gamma\gamma$ candidates at the χ_2 and for the background data taken at $\sqrt{s} \approx 3525\ MeV$ (scaled to the luminosity taken at the χ_2 and corrected for the energy dependence of the background). The expected angular distribution for $\bar{p}p \rightarrow \chi_2 \rightarrow \gamma\gamma$ events, discussed below, is shown in the inset. Due to the rapid increase of the background with $|cos\theta^*|$, the acceptance is restricted to the region $|cos\theta^*| \leq 0.40$. Various values of this cut from $|cos\theta^*| \leq 0.25$ to $|cos\theta^*| \leq 0.50$ give consistent results.

The results of this analysis are reported in table I and displayed in Fig. 4. The data taken at $\sqrt{s} \approx 3525\ MeV$ have been combined in table I and Fig. 4.

A maximum likelihood analysis of the data was performed using a power law dependence for the background, $\sigma_{\text{bkgr.}} = A(\sqrt{s})^B$ and a Breit-Wigner line shape convoluted with the beam energy distribution. The data were fitted for the background parameters, A and B, and for the parameter $\sigma = \frac{5\pi}{k^2} BR_{\text{in}} BR_{\text{out}} \times$ *efficiency* $\times$ *acceptance*. The mass and total width of the resonance were fixed at $M = 3556.15\ MeV$ and $\Gamma = 1.98\ MeV$, the values obtained from our analysis of the radiative decay $\chi_2 \rightarrow J/\psi\ \gamma$ [2]. The results are:

$$\sigma_{\text{bkgr.}} = (11.8 \pm 0.7\ pb) \times \left[\frac{3556\ MeV}{\sqrt{s}}\right]^{7.3 \pm 4.8} \tag{2}$$

$$\sigma = 14.8 \pm 3.6 \pm 0.5\ pb. \tag{3}$$

The systematic error in σ reflects the uncertainty in the mass and total width of the χ_2 resonance and the uncertainty in the absolute scale of the beam energy, $\approx \pm 120\ KeV$. The data and fitted curve in the χ_2 region are shown in the inset in Fig. 4.

The analysis efficiency has been measured using background free samples of $\psi' \rightarrow e^+e^-$ and $J/\psi \rightarrow e^+e^-$ events, selected using the hodoscopes and the Čerenkov data. These events are indistinguishable from $\gamma\gamma$ events in the calorimeter. The efficiencies calculated from the ψ' and two ψ samples are in good agreement. The efficiency of the analysis of these data, prior to the acceptance cut, is $\epsilon_{\rm analysis} = 0.79 \pm 0.02 \pm 0.04$. The overall efficiency is $\epsilon = \epsilon_{\rm trigger} \times \epsilon_{\rm analysis} = 0.72 \pm 0.04 \pm 0.06$.

The angular distribution for the reaction $\bar{p}p \to \chi_2 \to \gamma\gamma$ is needed in order to extract the partial width $\Gamma(\chi_2 \to \gamma\gamma)$ from a measurement over the restricted angular region $|cos\theta^*| \leq 0.40$. Due to the limited statistics of the data and the strong angular dependence of the background we are unable to extract the angular distribution directly. From the analysis of the reaction $\bar{p}p \to \chi_2 \to J/\psi\ \gamma \to e^+e^-\ \gamma$ [5] we find that the initial state is dominated by helicity=1, with an upper limit (95% CL) of 20% for the helicity=0 component. Non-relativistic models predict that the decay, $\chi_2 \to \gamma\gamma$, is purely helicity=2. With relativistic corrections the helicity=0 component is predicted to be $\leq 5\%$ of the partial width [6, 7]. If we assume pure helicity=1 in the initial state and pure helicity=2 in the final state then the angular distribution assumes the simple form $W(\theta^*) = (5/4)[1 - cos^4\theta^*]$. Integrating over $|cos\theta^*| \leq 0.4$, the fraction of the total cross section observed is 0.50 ± 0.02, where the estimated error is associated with the uncertainties in the neglected helicity=0 components.

Correcting our results for efficiency and acceptance we find that

$$BR(\chi_2 \to \bar{p}p)BR(\chi_2 \to \gamma\gamma) = (1.54 \pm 0.38 \pm 0.14) \times 10^{-8} \tag{4}$$

$$BR(\chi_2 \to \gamma\gamma) = (1.54 \pm 0.40 \pm 0.24) \times 10^{-4} \tag{5}$$

$$\Gamma(\chi_2 \to \gamma\gamma) = (304 \pm 84 \pm 49)\ eV. \tag{6}$$

We have used this experiment's measurements of $BR(\chi_2 \to \bar{p}p) = (1.00 \pm 0.09 \pm 0.13) \times 10^{-4}$ and $\Gamma(\chi_2) = 1.98 \pm 0.17 \pm 0.07\ MeV$ [2, 8] to obtain the last two values. A comparison of our results with previous measurements and with theoretical predictions appears in table II.

Perturbative QCD expressions for the decay rates of charmonium into gluons and photons with next-to-lowest order corrections can be found in Ref. [1]. The strong coupling constant $\alpha_s(m_c)$ can be derived from the ratio

$$\frac{\Gamma(\chi_2 \to gg)}{\Gamma(\chi_2 \to \gamma\gamma)} = \frac{9\alpha_s^2}{8\alpha^2}\left[\frac{1-2.2\alpha_s/\pi}{1-16\alpha_s/3\pi}\right]. \tag{7}$$

Using this measurement of the $\gamma\gamma$ width and our value of $\Gamma(\chi_2 \to gg) = 1.71 \pm 0.21\ MeV$ [2], a value $\alpha_s(m_c) = 0.36 \pm 0.04$ is obtained from the expression above. It should be noted that the lowest order correction to the two photon rate of the χ_2 is very large, $[1 - 16\alpha_s/3\pi] = 0.49$ for $\alpha_s = 0.3$ and that potentially large relativistic corrections have not been taken into account.

REFERENCES

[1] W. Kwong *et al.,* Phys. Rev. D **37**, 3210 (1988) and references therein.
[2] T. A. Armstrong *et al.,* Nucl. Phys. B **373**, 35 (1992).
[3] L. Bartoszek *et al.,* Nucl. Instrum. Methods **A301**, 47 (1991).
[4] R. Ray *et al.,* Nucl. Instrum. Methods **A307**, 254 (1991).
[5] T. A. Armstrong, (to be published).
[6] Z. P. Li *et al.,* Phys. Rev. D **43**, 2161 (1991).
[7] T. Barnes and E. Ackleh, ORNL-CCIP-92-05, UTK-92-3
[8] Particle Data Group, "Review of Particle Properties," Phys. Rev. D **45**, S1 (1992).
[9] C. Baglin *et al.,* Phys. Lett. B **187**, 191 (1987).
[10] W. Chen *et al.,* Phys. Lett. B **243**, 169 (1990).
[11] H. Aihara *et al.,* Phys. Rev. Lett. **60**, 2355 (1988).
[12] G. Bodwin *et al.,* Phys. Rev. D **46**, 1914 (1992).

TABLES

TABLE I. Final $\gamma\gamma$ candidates.

$\sqrt{s}$ (MeV)	Events	$\int \mathcal{L}$ (pb^{-1})	Events/$\int \mathcal{L}$ (pb)
3522.7-3527.0	204	15.893	12.8
3555.3	7	0.304	23.0
3555.9	55	2.103	26.2
3556.6	2	0.169	11.8
3590.8	9	0.924	9.7
3594.6	5	0.827	6.0
3612.8	5	1.167	4.3
3615.9	13	1.276	10.2
3618.9	7	0.575	12.2
3621.1	16	1.216	13.2
3667.7	2	0.372	5.4
3686.0	14	0.995	14.1

TABLE II. Comparison with other measurements and theory.

	$\Gamma(\chi_2 \rightarrow \gamma\gamma)$ (KeV)	$BR(\chi_2 \rightarrow \gamma\gamma)$ (10^{-4})
Experiment		
E760	$0.30 \pm 0.08 \pm 0.05$	$1.5 \pm 0.4 \pm 0.2$
R-704 [9]	$2.9^{+1.3}_{-1.0} \pm 1.7$[a]	$11^{+5}_{-4} \pm 4$[a]
CLEO [10]	< 1.0 (95% CL)	
TPC [11]	< 4.2 (95% CL)	
DASP [8]	< 1.6 (90% CL)	
Theory		
PQCD [1]	0.70 ± 0.13[b]	
B.A. [7]	0.56	
B.B.L. [12]		4.1 ± 1.1 ($\pm 36\%$)

[a] Uses isotropic angular distribution and $\Gamma(\chi_2) = 2.6^{+1.4}_{-1.0}$ MeV.

[b] Using $\Gamma(\chi_2 \rightarrow gg) = 1.71 \pm 0.21$ MeV.

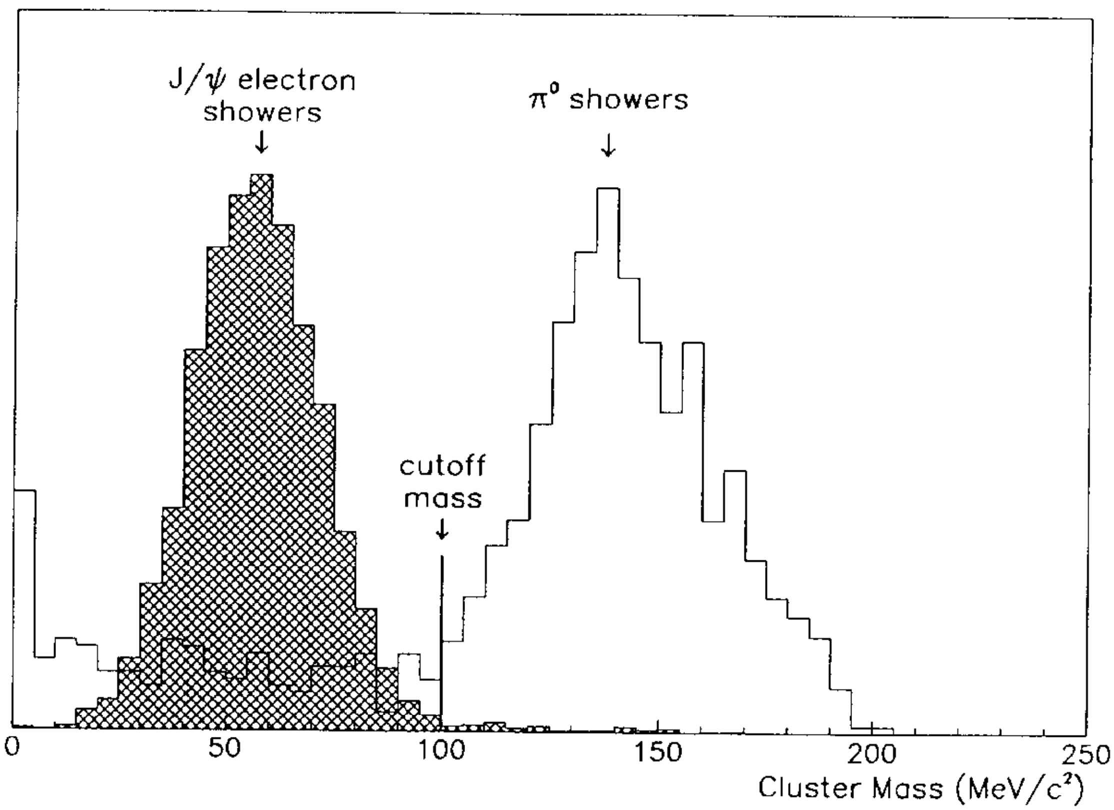

FIG. 1. Cluster *mass* of showers in the calorimeter.

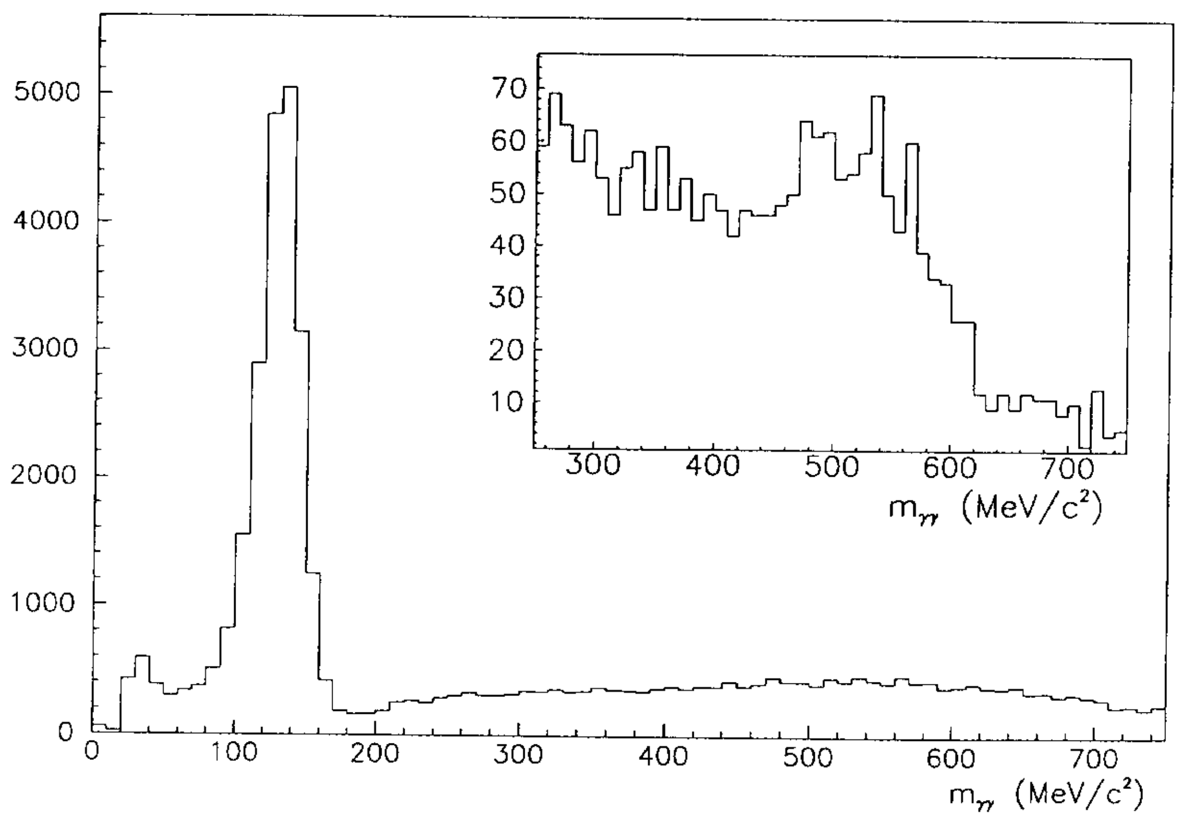

FIG. 2. Invariant mass of extra clusters with $\gamma\gamma$ candidate clusters.

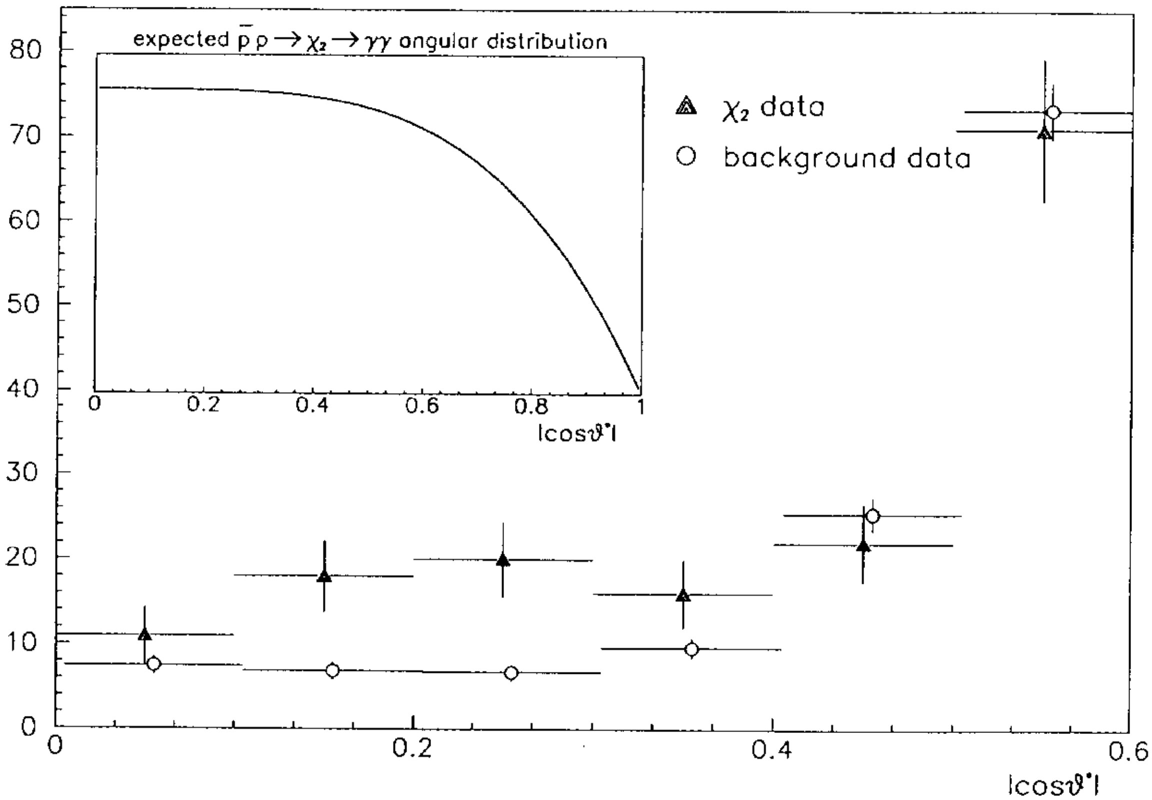

FIG. 3. Center of mass angular distribution of $\gamma\gamma$ candidates.

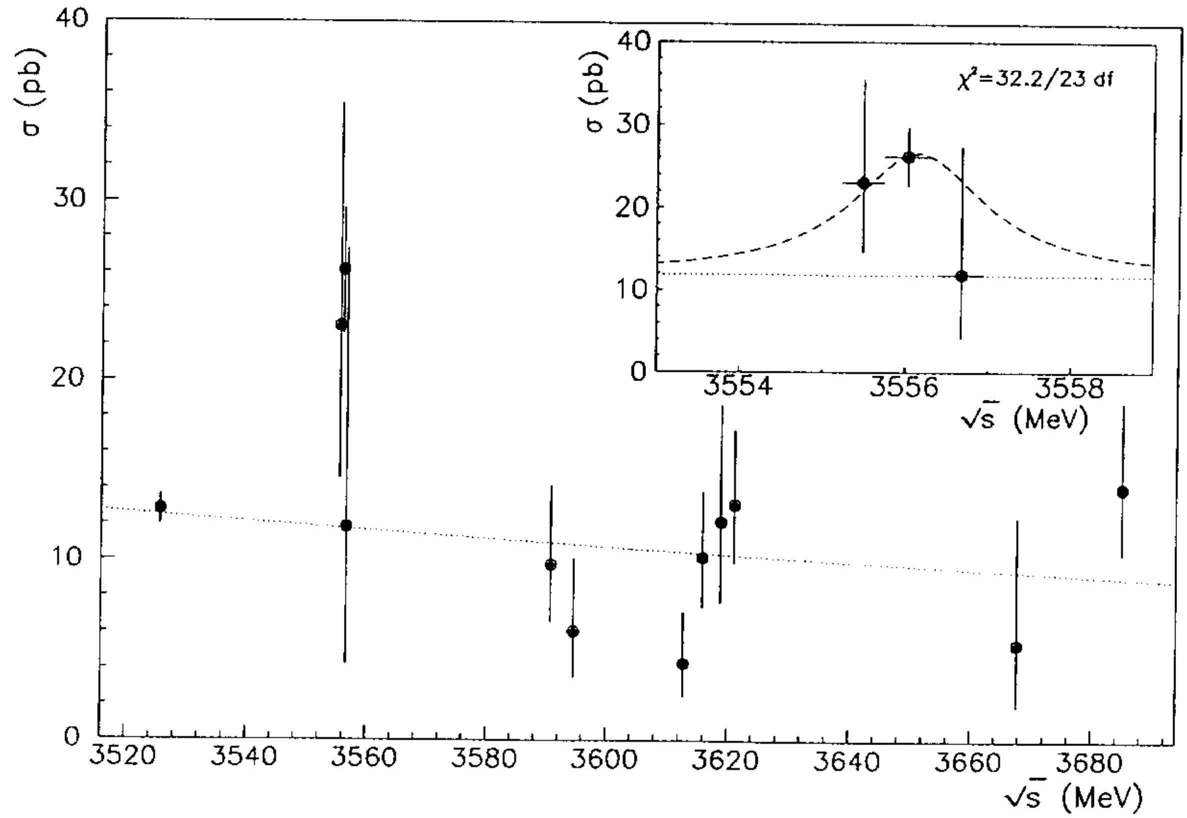

FIG. 4. Measured $\gamma\gamma$ cross section for the final data set (not corrected for efficiency and acceptance).